Magnification of Tsunami Risks Due to Sea Level Rise Along the Eastern Coastline of Japan

Kentaro Koyano[1], Tomoyuki Takabatake[2], Miguel Esteban[3] and Tomoya Shibayama[4]

Abstract

Sea level rise is likely to increase the risks of inundation due to coastal hazards in the course of the 21st century. To understand how different sea level rise (SLR) scenarios will affect the disaster risk management of tsunamis in Japan, the authors applied the Probabilistic Tsunami Hazard Assessment (PTHA), using a logic tree approach, to the eastern coastline of Japan. Considering a similar generation zone as the *2011 Tohoku Earthquake and Tsunami*, a number of tsunami propagation simulations were conducted. In the logic tree construction, different branches of magnitude ranges, positions of asperity, recurrence intervals, standard deviations of log-normal distribution and truncations of log-normal distribution were set. The results indicate that the maximum water levels at output points increased according to the different SLR scenarios that were considered. It was also found that the effects that SLR has on expected tsunami heights and 90% confidence intervals are nonlinear and could vary according to location. Such results highlighted the importance of considering the effects of SLR to improve emergency response capacity.

Keywords

Tsunami, Sea Level Rise, Climate Change, Hazard Assessment, Simulations, Probabilistic Tsunami Design

[1]k10900530@asagi.waseda.jp, Waseda University, Tokyo, Japan
[2]takabatake@civileng.kindai.ac.jp, Kindai University, Osaka, Japan
[3]esteban.fagan@gmail.com, Waseda University, Tokyo, Japan
[4]shibayama@waseda.jp, Waseda University, Tokyo, Japan

1   Introduction

Tsunamis constitute some of the most dangerous types of natural hazards, often devastating coastal areas exposed to them. For instance, the 2004 Indian Ocean Tsunami, with an estimated Moment Magnitude Mw of 9.3, caused widespread destruction to countries around the Indian Ocean, resulting in more than 1,126,00 displaced, and 283,000 casualties (Spence et al., 2009). The 2011 Tohoku Earthquake and Tsunami significantly damaged the Pacific coastline of Japan, causing an estimated 25,000 casualties and over 41,000 people being displaced (National Police Agency of Japan, 2020). Other more recent events include the 2018 Sulawesi Tsunami, caused by an earthquake which affected Palu Bay in Indonesia (Mikami et al., 2019; Harnantyari et al., 2020), and the 2018 Sunda Straight tsunami, generated by the flank collapse of the Anak Krakatau volcano (Takabatake et al., 2019a).

The conventional method of assessing the risk of tsunamis focuses on the analysis of the worst-case scenario of historical events that have taken place in a given area (Teh et al., 2011). More recent approaches involve the probabilistic estimation of the potential return periods of different inundation heights, using methods such as the Probabilistic Tsunami Hazard Assessment (PTHA, see for example Becerra et al., 2020 and Park et al., 2017). Through such methods, the expected inundation extent, casualties and total financial damage can be estimated in a probabilistic manner, allowing coastal risk managers to formulate appropriate countermeasures. The PTHA has been more actively studied after the 2011 Tohoku Earthquake and Tsunami. Prior to this event the risk management of earthquakes and tsunamis along the eastern part of Tohoku (Iwate, Miyagi, Fukushima Prefectures) and Kanto Regions (Chiba, Ibaraki Prefectures) of the country were formulated by analyzing historical earthquakes at the northern part of the Japan Trench. However, the actual rupture length of the fault in 2011 extended from the northern part to the southern half of the Japan Trench, generating a larger tsunami than expected (The Central Disaster Management Council (CDMC), 2011). As a consequence of this, the Japanese coastal engineering community established two levels of tsunami design, and the idea that hard measures along the coastline can always protect human society against tsunamis has been abandoned (Shibayama et al., 2013). Level 1 tsunamis are events with a return period of several decades up to around 100 years, with coastal structures being designed to protect people and their property against such events. Level 2 tsunamis have a return period in the order of 1000 years, and evacuation measures should be designed to ensure that all residents can safely escape even in the case that such inundation takes place.

Following this reclassification of potential tsunami events, a number of PTHA along the coastline of the Tohoku and Kanto Region have been conducted (see Goda et al., 2016; Mori, et al., 2017; Kotani et al., 2020). For instance, Fukutani et al. (2018) made an assessment of the uncertainty in tsunami heights by using a random source parameter model based on the 2011 Tohoku Earthquake. As a result, they attempted to establish the return period of this type of earthquake by comparing it with the actual tsunami heights at a tide gauge off the southern Iwate coast. Goda et al. (2014) developed stochastic random-field slip models for the 2011 Tohoku Earthquake for e evaluating tsunami hazards due to future mega-thrust events. Annaka et al. (2007) constructed tsunami hazard curves to evaluate the risk to nuclear power facilities at Fukushima prefecture by using a PTHA with a logic-tree approach. Sugino et al. (2014) clarified the effects of simultaneous and independent rupture processes on the PTHA, and introduced new branches of rupture processes to advance the logic tree approach. Nobuoka et al. (2017) compared the capacities of a Gutenberg-Richter (GR) model, logic tree-approach and extreme value theory with observed records by estimating the tsunami hazard along the coastline of Ibaraki Prefecture in Japan, indicating that the logic tree method showed good agreement with the design height of sea walls and hazard areas determined by expert judgements for the prefecture.

A PTHA that uses a logic-tree approach can help to elucidate uncertainty regarding the tsunami heights that can be generated by a given source zone, helping to assess the risk of these disasters in the future. There are a few studies that have mentioned the effect of tidal heights on future tsunamis estimated by PTHA methods (see for example Adams et al., 2014 and Lane et al., 2014). However, to the authors' best knowledge, when performing such exercises, very little research has considered the influence that sea-level rise (SLR) will have on the overall risk (some exceptions to this being the work of Arnoud et al. (2021) on how tsunamis originating from La Palma volcano could affect Guadeloupe, and Tursina et al. (2021) on the impact of SLR on future tsunamis in Banda Aceh). The Intergovernmental Panel on Climate Change (IPCC) 5th Assessment Report (Church et al., 2013) concluded that sea levels have been rising by over 3 mm per year since 1992, and could be 0.26 - 0.82 m higher than at the present by the year 2100. As this projection is higher than that in the previous IPCC AR4 (0.18-0.59 m), it is likely that future estimates will continue to be raised as the scientific community's understanding of how the planet works gradually improves. The signing of the Paris Agreement in 2015, as part of the United Nations Framework Convention on Climate Change (UNFCCC), has created expectations that greenhouse gas emission will be gradually curtailed, though there is at present little evidence of a long-term reduction materializing. Moreover, a number of studies using probabilistic process-based models indicate that the Antarctic ice sheets could melt rapidly under Representative Concentration Pathway (RCP) 8.5, leading to SLR of 2.97 -3.39 m by the year 2100 (Kopp et al., 2017).

As stated earlier, to the authors' knowledge there is little literature that has considered the issue of future SLR when evaluating tsunami hazards. Wang et al. (2016) estimated the tsunami inundation risk to Macau City, which will significantly increase even with a minor amount of SLR (+0.5 m). Li et al. (2018) also estimated the variation of inundation depths around Macau City by using a numerical simulation of different earthquake and tsunamis for +0.5 m to +1.0 m SLR scenarios, and concluded that 0.5 m SLR could double the tsunami hazard in Macau City. Nagai et al.

(2020) investigated the effects of SLR on the extent of the estimated inundation area and velocity of the water in Tokyo Bay under extreme tsunami scenarios, and indicated that the risk of casualties would greatly increase when SLR exceeds +1.0 m. However, such scenarios did not consider the influence that SLR will have on hazard risks caused by a Japan Trench megathrust. As this subduction zone could potentially cause future tsunamis, there is a need to understand how SLR by the end of the century will affect the improved countermeasures that have been built along the Pacific coastline of Japan following the 2011 Tohoku Earthquake and Tsunami. While this approach is in line with other studies considering tide uncertainties (Adams et al., 2014, Lane et al., 2012), there is some merit in isolating the effect of SLR, in order to focus attention on possible non-linear effects that may influence adaptation strategies for tsunami countermeasures. Thus, the objective of the present study is to conduct a probabilistic tsunami hazard assessment of the 2011 Tohoku Earthquake type tsunamis (essentially, looking at the same fault line that generated the 2011 Tohoku Earthquake), but taking into account different SLR scenarios. The 2011 Tohoku Earthquake and Tsunami caused significant damage along the coastline of the Tohoku and Kanto regions, including Kujukuri Beach, as shown Figure 1 (which is located on the northeast side of the Boso Peninsula in Chiba prefecture, about 350 km away from the epicenter of this earthquake). The first tsunami wave (8.7 m in high) arrived at the Nakayari District in Asahi City about 60 mins after the earthquake, and larger waves were observed 150 min after the earthquake (The 2011 Tohoku Earthquake Tsunami Joint Survey (TTJS) Group, 2012), resulting in over 270 casualties (Department of Disaster Management of Chiba Prefecture, 2015). As Kujukuri Beach has an arc-shape and extends over 45 km, there is some indication that the tsunami waves propagated as edge waves along the continental shelf, enhancing the damage that took place (Koyano et al., 2021). Such complex wave phenomena and the damage that resulted from it highlights the importance of studying tsunami behavior to protect human settlements in the area. In addition, the tsunami hazard along the coastline of the Tohoku Region (near Sendai new port) was also estimated to provide a comparison with the results at Kujukuri Beach. Ultimately, considering the evolution of tsunami hazards as SLR progresses in the course of the 21st century can help risk managers to plan the gradual improvement of coastal defenses along this coastline, in order to improve the resilience of the coastal communities they serve.
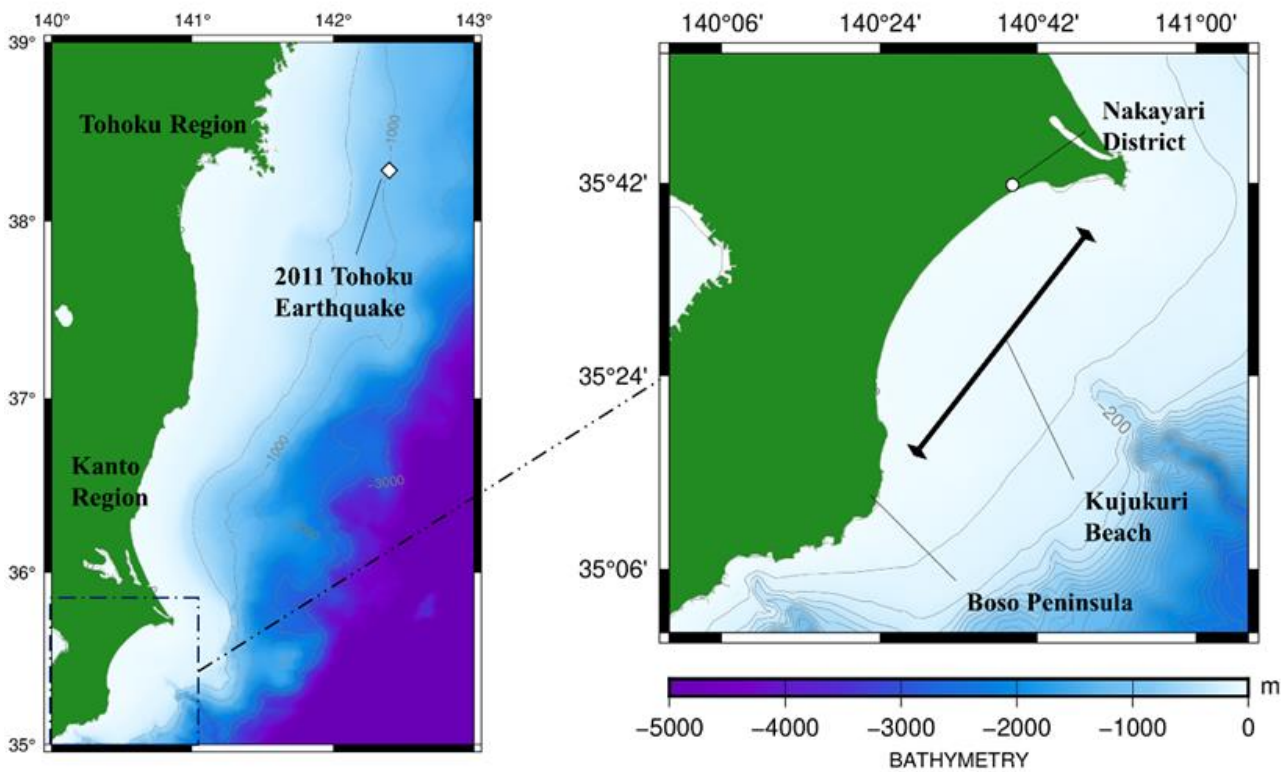

Figure 1. Map of the location of the target earthquakes, the coastline of Kujukuri Beach and Boso Peninsula, Japan

2   Methods

2.1. Probabilistic Tsunami Hazard Assessment(PTHA)

PTHA methods can be used to analyze the variation and probability of maximum run-up and inundation heights for a certain return period of target earthquakes zones by modeling the uncertainty in the source and rupture process. PTHA is based on the methodology of Probabilistic Seismic Hazard Analysis (PSHA), which models uncertainties regarding earthquake magnitudes and their attenuations probabilistically, assuming a relationship between the maximum accelerations of the ground motion and return periods (Cornell, 1968).

There are mainly two different methodologies that can be used to conduct a PTHA: the random phase method and the logic-tree method (see Annaka, 2007; Fukutani et al., 2018). The random phase method creates stochastic slip distributions following the inversion modeling of fault slips that previously occurred to evaluate tsunami hazards. This method can clarify the correlation between the distribution of fault slips and tsunami heights, though other factors related with the uncertainty in fault parameters and tsunami heights (such as interval occurrences) are difficult to consider using this method (see Fukutani et al., 2018). The logic-tree method can classify uncertainties in tsunami models into aleatory and epistemic categories and evaluate the probability distribution of expected tsunami heights. Aleatory uncertainty is caused by randomness in the natural phenomena (i.e., the range of the potential magnitudes), whereas the epistemic uncertainty originates from a lack of accurate data regarding the position of the epicenter, range and length of the faults. Comprehensive results can be estimated by averaging the results from each scenario based on the logic tree construction. In Japan, a subcommittee of the Japan Society of Civil Engineers (JSCE) has been established in order to upgrade and propose safety assessment techniques for nuclear power plants against tsunamis. The logic tree method has been introduced as an example of PTHA methods in the technical reference books on tsunamis published by this committee (JSCE, 2006, 2011, 2016). The logic-tree method was also adopted in the PTHA for future Nankai-Tonankai Earthquake Tsunamis, conducted by the Headquarters for Earthquake Research Promotion in Japan (2020). As the logic-tree method has advantages in terms of its simplicity to determine source parameters, it has also been widely used in academic research (e.g., Fukutani et al. 2014, 2015; Sugino et al., 2015; Park and Cox, 2016; Nobuoka and Nogami, 2017). As the framework of the logic-tree method has been formulated based on that of the PSHA, it is relatively easy to combine these two methods and conduct a multi-hazard risk assessment, which is another advantage of the logic-tree method. For instance, Park et al. (2019) conducted a probabilistic seismic and tsunami damage analysis of buildings in their study area by extending the logic-tree model proposed in Park and Cox (2016). Figure 2 presents a logical diagram that illustrates the steps to compute the fractile curves of tsunami heights by using the logic-tree method. Firstly, the earthquake fault source model and its characteristics are defined to create a logic tree construction, which determines the various displacement parameters. Subsequently, a tsunami source model is created and various SLR scenarios are formulated, which are then computed using a numerical simulation model based on the non-linear long wave equations. Consequently, the relationship between annual exceedance probability curves of tsunami heights and the cumulative weights of the branches can be obtained.

In the present study the authors selected the logic tree method to analyze the uncertainty in tsunami height distribution along Sendai New-port and the Kujukuri Beach. The general approach used follows the work of Annaka et al. (2007), where the aleatory uncertainty was determined from Aida's Kappa (Aida, 1978), which was obtained by calculating the ratios of observed to numerically calculated tsunami heights for eleven historical tsunami sources. To construct the logic tree the various rules that govern it (i.e., the ratio of the weights of branches, or the type of branches) were defined in reference to previous work, as will be detailed in the following section. The branches were made for a combination of tsunami generation zones, the magnitude and interval occurrence of characteristic earthquakes for each tsunami generation zones, and the error in the estimation value. The weights of the branches were determined based on a questionnaire survey of tsunami and earthquake experts and an error evaluation (Annaka et al., 2007; Japan Society of Civil Engineers (JSCE), 2008). It is worth mentioning that the necessity of assigning a weight to each of the branches is one of the disadvantages of the logic-tree method, as this requires considerable effort in practice and might be influenced by the subjectivity of each expert. In contrast, the random phase method can randomly generate the asperity distribution and Mw of a target earthquake, which can appear to be more scientifically justified. However, as mentioned earlier, it is not easy for the

random phase method to account for uncertainties in earthquakes other than the distribution of the asperity and the variations in Mw.

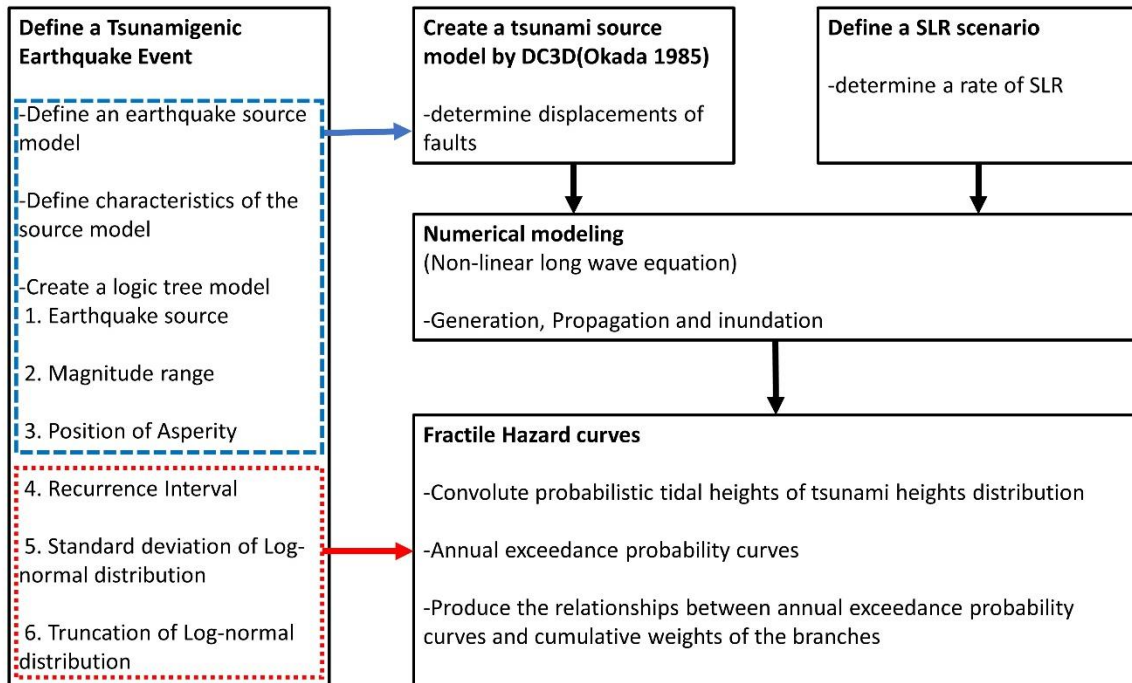**Probabilistic Tsunami Hazard Assessment**

Define a Tsunamigenic Earthquake Event	Create a tsunami source model by DC3D(Okada 1985)	Define a SLR scenario
-Define an earthquake source model	-determine displacements of faults	-determine a rate of SLR
-Define characteristics of the source model		
-Create a logic tree model		
1. Earthquake source	**Numerical modeling** (Non-linear long wave equation)	
2. Magnitude range	-Generation, Propagation and inundation	
3. Position of Asperity		
4. Recurrence Interval	**Fractile Hazard curves**	
5. Standard deviation of Log-normal distribution	-Convolute probabilistic tidal heights of tsunami heights distribution	
6. Truncation of Log-normal distribution	-Annual exceedance probability curves	
	-Produce the relationships between annual exceedance probability curves and cumulative weights of the branches	

Figure 2. Logical diagram of the methodology followed in the present study

2.2. Logic tree construction

To stochastically analyze the tsunami hazard the authors constructed a logic tree with five branch levels (namely the range of moment magnitude, position of asperity, earthquake return period, log normal standard deviation expressed as aleatory uncertainty, and truncated uncertainty), based on Annaka et al. (2007).

Figure 3 shows the logic tree construction for the 2011 Tohoku Earthquake. The range of Mw was varied by ±0.1 from the actual magnitude of the 2011 Tohoku Earthquake (Mw 9.0), following available literature (see Youngs & Coppersmith, 1985; JSCE, 2008; Fukutani et al., 2014). Another important parameter to be considered is the asperity, which Somerville et al. (1999) defined as the region having a slip which is at least 150% greater than the average slip across the fault. Following the works of Annaka et al. (2007) and Nobuoka et al. (2017), the asperity positions were determined to be located on the northern, the central and the southern part of this fault. The distribution of the slip displacements and the fault area were determined according to Sugino et al. (2014), as will be explained later.

The return period for the 2011 Tohoku level earthquake was estimated considering a Brownian Passage Time (BPT) distribution, with three branches which show the average, lower and upper limits of the recurrence interval1. Previous studies (NIED, 2013; Fujiwara et al., 2013) indicated that this level of earthquake has occurred 4 times in the last 2,400 years, with an average return period of 600 years. By using this information and assuming the deviation of the BPT

---

[1] A BPT curve in itself is not related to any specific seismic parameter, although this curve can be created by using the average occurrence of an earthquake and the parameter of dispersion. These parameters were based on previous studies (NIED, 2013; Fujiwara et. al., 2013). A BPT is used to determine the return periods in this study, which is not related to the determination of the various tsunami source models. The variety of tsunami source models was determined according to the earthquake source type, range of magnitudes and asperity. Note also that in the present study the range of the magnitude is so large that all cases could generate tsunamis.

distribution to be 0.3, the lower and upper limits of the recurrence interval were determined (532 years and 676 years, respectively).

The branches of the standard deviation of the log-normal distribution were adopted to consider the uncertainty in the simulated tsunami heights[2]. This idea is based on the assumption that the actual tsunami height would be located within the errors obtained from the logarithmic standard deviation and simulated tsunami height (Aida, 1978). However, as the error between the actual and simulated tsunami heights would not be extremely small and large, the last branches were set to ignore the extreme values obtained from the log-normal distribution of the tsunami heights. The values proposed in Annaka et al. (2007) were adopted for the standard deviation of log-normal distribution and truncation in the present study.

The numbers indicated on each of the branches in Figure 3 are their respective weights. Following previous works (Annaka et al., 2007; JSCE, 2008), the sum of weights in the logic-tree equals 1.0. The weights of the branches on the Mw range and the position of the asperity were divided equally, and the weight of the average return period and the other return periods were set to 0.5 and 0.25, respectively. For the weights on the branches of the standard deviation of log-normal distribution and the truncation, the same values as those in Annaka et al. (2007) were adopted.
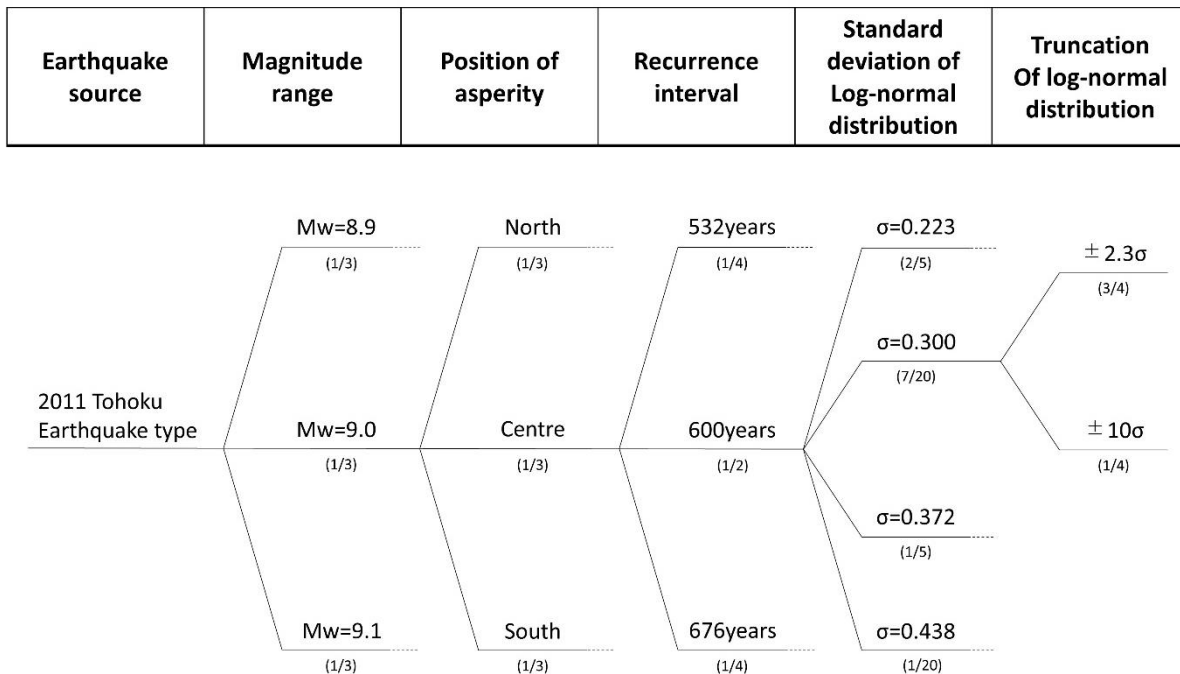
Earthquake source	Magnitude range	Position of asperity	Recurrence interval	Standard deviation of Log-normal distribution	Truncation Of log-normal distribution

Figure 3. Logic tree construction. The numbers attached to each branch indicate its weight. The position of asperity of "north" indicates an earthquake situated in the northern section of the Japan Trench (roughly northern offshore of Iwate prefecture); centre indicates an earthquake offshore of Iwate, Sendai and Fukushima prefectures, and south of Fukushima and Ibaraki prefectures.

2.3. Tsunami source model

Tsunami source models were created following the logic tree. The parameters used to model the 2011 Tohoku-level earthquake were based on Satake-Fuji model ver. 4.2 (Fujii et al., 2011). It should be noted that the authors only considered vertical displacement of the faults to calculate the initial water surface profile (i.e. neglected the effects of horizontal displacement) for the sake of simplicity, as Koyano et al. (2021) confirmed that the vertical displacement could

---

[2] Following Annaka et al. (2007), the present study assumed that the distribution of tsunami heights around the median value would follow a log-normal distribution. The standard deviation of the log-normal distribution σ, which is related to an error factor κ (often referred to as Aida's κ in Japan), given as $\kappa = \exp(\sigma)$ (Aida, 1978), was changed to account for different shapes of a log-normal distribution. In the present study, four values were adopted for σ (the same values adopted in Annaka [2007]), meaning that four branches were made in the logic-tree (see Figure 3).

reproduce sufficiently well the inundation heights recorded in the study area (Kujukuri Beach) and actual waveform recorded at the wave gauge near this beach during the *2011 Tohoku Earthquake and Tsunami*. Essentially, the branches from the logic-tree (except the part relating to the recurrence interval, standard deviation of a log normal distribution and truncation of a log normal distribution) determined the displacement through the parameters of moment magnitudes and asperity. The moment magnitude is used to determine how much the fault area slips (average displacement), and the asperity is used to determine the distribution of the slip amount over the entire fault area (following Sugino et. al., 2014).

The average displacement across the fault *D* was determined by using Eqs. (1) and (2), which were derived from the scaling law of earthquakes (Eshelby, 1957).

$$D = \frac{M_0}{\omega S} \tag{1}$$

$$M_0 = 10^{1.5M_w + 9.1} \tag{2}$$

where M_0 is the seismic moment (N·m), ω refers to modulus of rigidity (=4.0×10^{10} N/m²), S and M_w represent the fault area (k$_m$) and the moment magnitude (N·m), respectively. The slip amount was distributed unevenly over the entire fault area by following Sugino et al. (2014), who determined the parameters of faults areas and slips based on existing tsunami source models of historical inter-plate earthquake. Specifically, as the magnitude and fault area of the *2011 Tohoku Earthquake* was rather large, three different slip values (which correspond to small, large and extreme large fault slips, respectively) were distributed over the entire fault area, with values of 0.33D, 1.4D and 3D, respectively. For the size of the fault area of each slip, 0.6S was used for small fault slip and 0.25S and 0.15S were used for the large and extreme large fault slips (Sugino et al., 2014). As large fault slips are known to have taken place near the Japan Trench during *2011 Tohoku Earthquake and Tsunami* (Fukutani et al., 2014), the large and extreme large slips were distributed along the sea trench to limit conceivable cases of the fault distribution. After determining the fault slip distribution, the initial water level for each earthquake scenario was calculated using the formulas proposed by Okada (1985), with Figure 4 showing an example of the slip distribution and an example of the calculated initial water level.
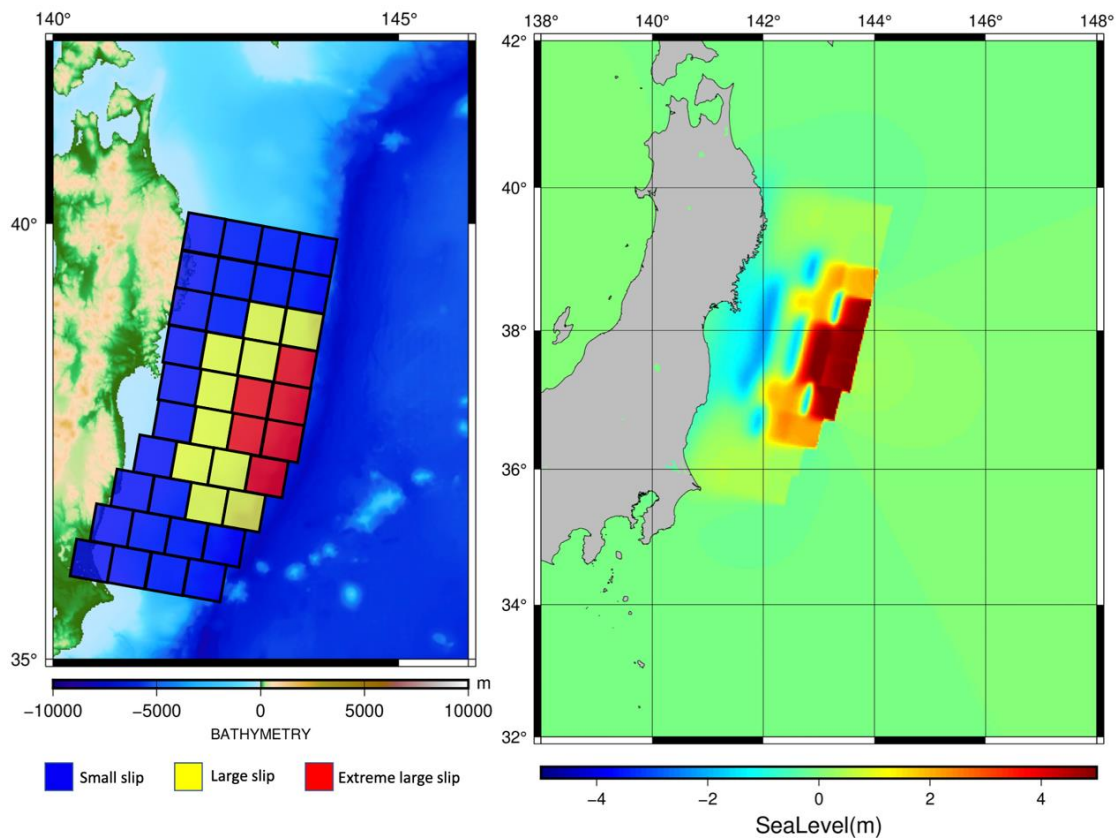

Figure 4. Left) Location of the fault model Right) An example of the tsunami source model (in this case, the M$_w$ 9.0 is used and the asperity of the earthquake is located in the centre of the fault model).

2.4. Sea level rise

In the present work, the authors used 6 different sea level rise scenarios (0 m to +2.5 m), as shown in Table 1. The percentages in Table 1 correspond to the probability that they will be exceeded by 2100, as assessed using the RCP-based probabilistic projections (see Kopp et al., 2014), which assumed that the rate of ice-sheet mass loss will increase with a constant acceleration in the future. The Low and High scenarios have a 49% to 96% and a 0.05% to 0.1% chance of being exceeded under RCP 2.6 and RCP 8.5, respectively. However, Kopp et al. (2014) mentioned that the probability of the Intermediate, Inter-High and High scenarios may significantly increase. Although these scenarios - especially the Intermediate-High and High cases - might not materialize, the authors would nevertheless like to stress that envisaging these worst-case SLR scenarios can help to conceptualize the range of adaptation measures that disaster risk managers need to contemplate.

Table 1. SLR Scenarios, indicating the probability of exceedance for RCP2.6, RCP4.5 and RCP8.5 (see Kopp et al., 2014).

SLR Scenario	RCP2.6	RCP4.5	RCP8.5
0m(present day)	-	-	-
0.5m	49%	73%	96%
1.0m	2%	3%	17%
1.5m	0.40%	0.50%	1.30%
2.0m	0.10%	0.10%	0.30%
2.5m	0.05%	0.05%	0.10%

2.5. Numerical simulation

A numerical method of tsunami simulation, which employed the nonlinear long wave equations with a Leap-Frog Scheme, was used to simulate tsunami propagation, as shown below in Eqs. (3)-(5).

$$\frac{\partial \eta}{\partial t} + \frac{\partial M}{\partial x} + \frac{\partial N}{\partial y} = 0 \tag{3}$$

$$\frac{\partial M}{\partial t} + \frac{\partial}{\partial x}\left(\frac{M^2}{D}\right) + \frac{\partial}{\partial y}\left(\frac{MN}{D}\right) + gD\frac{\partial \eta}{\partial x} + \frac{gn^2}{D^{7/3}}M\sqrt{M^2+N^2} = 0 \tag{4}$$

$$\frac{\partial N}{\partial t} + \frac{\partial}{\partial x}\left(\frac{MN}{D}\right) + \frac{\partial}{\partial y}\left(\frac{N^2}{D}\right) + gD\frac{\partial \eta}{\partial y} + \frac{gn^2}{D^{7/3}}M\sqrt{M^2+N^2} = 0 \tag{5}$$

where η is the water surface elevation, D refers to the total water depth, M and N represent the flux discharge in two horizontal directions, n is the Manning's roughness coefficient, and g is the acceleration due to gravity. The model was developed by the authors themselves following the study of Imamura (1989). This numerical model has been extensively verified elsewhere (Kukita and Shibayama, 2012; Takabatake et al., 2019b, 2020), and was shown to be able to accurately simulate the occurrence of edge waves along the coastline of the Kujukuri Beach during the *2011 Tohoku Earthquake and Tsunami* (Koyano et al., 2021).

In the present study the topography and bathymetry data, including a spatially distributed Manning's roughness coefficient that was different for each mesh cell, were assembled from the digital data set by CDMC (2006). The topography and bathymetry domains used a nesting approach that included 150 m (A3 and B3), 450 m (A2 and B2) and 1350 m (AB1) grid meshes (see Figure 5). The time step was set as 0.1 sec and the total computed time was 6 hours, as the tsunami waves originating offshore the Tohoku Region would take some time to travel along the coastline of Kujukuri Beach. SLR heights were set based on the mean sea level of Tokyo Bay(T.P.), and used into the initial condition of sea levels in this model. As tsunami heights along the coast are affected by tidal heights, the probabilistic density distribution of tidal heights was incorporated into this simulation by the convolution of tsunami heights distribution.
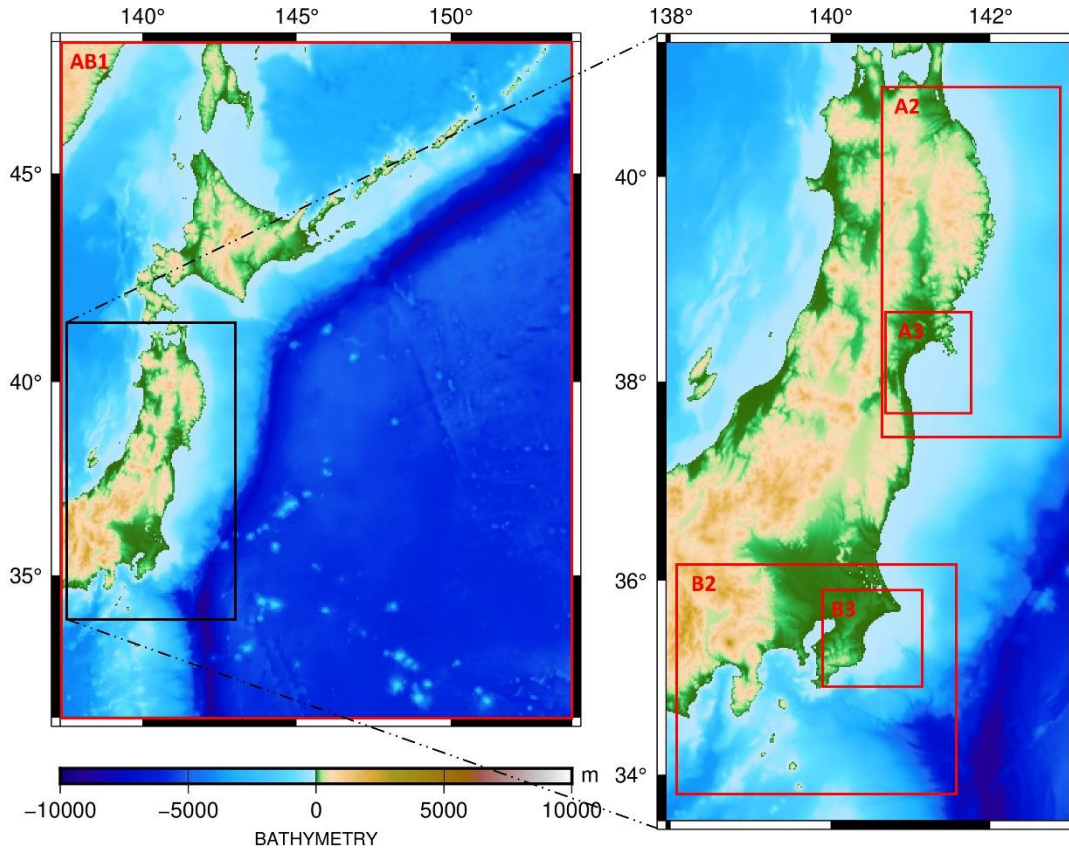
Figure 5. The nested domain (AB1-A3: Sendai Bay, AB1-B3: The Kujukuri Beach)

In computational domains A3 and B3, digital buoys at Sendai New-Port and Offshore of Asahi City were set at 10 m depths to compare the characteristics of near-field and mid-field (see Figure 6). During the *2011 Tohoku Earthquake and Tsunami*, the tide gauge point at Sendai New-Port recorded about a tsunami wave-height of 6.6 m (Kawai et al , 2013) before the tide gauge was broken. As a result, 4-8 m of runup heights were measured behind it (TTJS, 2012).
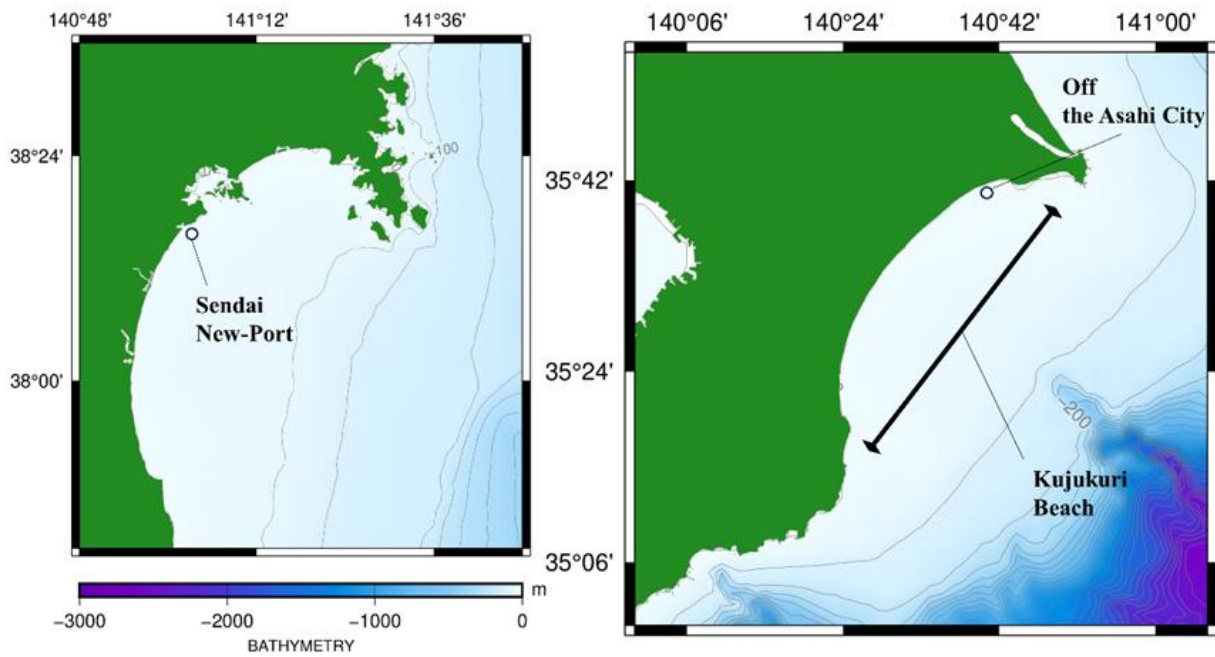
Figure 6. Location of digital wave buoys Left) at Sendai New-Port (NOWPHAS) and Right) Offshore Asahi City.

2.6. Fractile hazard curves

In the present study, fractile hazard curves were created to evaluate the annual probability of exceedance for tsunami heights (refer also to Appendix A for more details on these curves). According to the representation of an epistemic uncertainty, fractile hazard curves based on a Logic tree were created. Each of the fractile curves is created considering all the branches in a logic-tree, and the method to generate them starts by deriving the probability density function of a log-normal distribution for each branch of the logic tree, using Eq. (6). In this equation, the value x is a tsunami height, the median value μ takes the maximum tsunami height that is obtained through the numerical simulation of each branch, and the log-normal standard deviation (σ) is the logarithm of Aida's kappa for each branch, as shown in Figure 3.

$$f_{(x)} = \frac{1}{\sqrt{2\pi}\sigma x} \exp \left\{ \frac{-(logx - \mu)^2}{2\sigma^2} \right\} \qquad (6)$$

As the obtained probability density function could be converted to an exceedance probability distribution on the assumption of an ergodic hypothesis, tsunami hazard curves (which show the annual probably of exceedance according to a given tsunami height) corresponding to the number of all branches of the logic-tree could be obtained (thus, 216 curves were generated for each SLR scenario in the present study). Then, the relationship between the tsunami hazard curves and the cumulative weights of the branches for a given tsunami height could be produced. As the result, the fractile hazard curves were generated by connecting the probabilities with the same fractile values for different tsunami heights. In addition, evaluating arithmetic or simple average curves is also commonly used to determine representative heights of tsunami in the probabilistic model (see Yanagisawa et al., 2015; Fukutani et al., 2015).

3   Results

3.1 Time history of water surface elevations

In this section, the time history of water level at the digital water buoys off the Sendai New-Port and Asahi City, based on the numerical simulations of different asperity or SLR scenarios, are presented (See Figure 7). Here, the initial water level at present was set to be the standard level (0 m). At the digital water buoys off the Sendai New-Port, the maximum water level of the tsunami generated by an earthquake with an asperity located at the central part of the faults was 3.7 m and 4.1 m higher than in cases where the asperity was located at the northern or southern part of fault, as shown as Figure 7a. In contrast, the maximum water levels off Asahi City showed similar values (around 4.0 m) (see Figure 7b), though there were considerable differences in the tsunami arrival time. Due to the effects of SLR, the maximum water levels off Sendai New-Port increased by 1.4 m (+1.5 m SLR) to 2.2 m (+2.5 m SLR) (see Figure 7c), which means that the increase in maximum water level is slightly smaller than the increase in SLR. Essentially, the increase in initial water level would have a nonlinear effect on tsunami heights, as they will influence convection terms and friction losses in the governing equations (see Eqs. (4) and (5)). Also, it should be noted that there could also be some differences due to small changes in the geometry of the coastline due to this SLR. This clearly highlights the necessary to perform tsunami simulations to better understand the effects that SLR will have on potential future tsunami heights. The increase in the maximum water level off Asahi City was 0.1 m to 0.2 m greater than the 1.5 m and 2.5 m increased sea level (see Figure 7d). These results thus indicate how the effects of SLR on tsunami heights would likely be location-dependent.
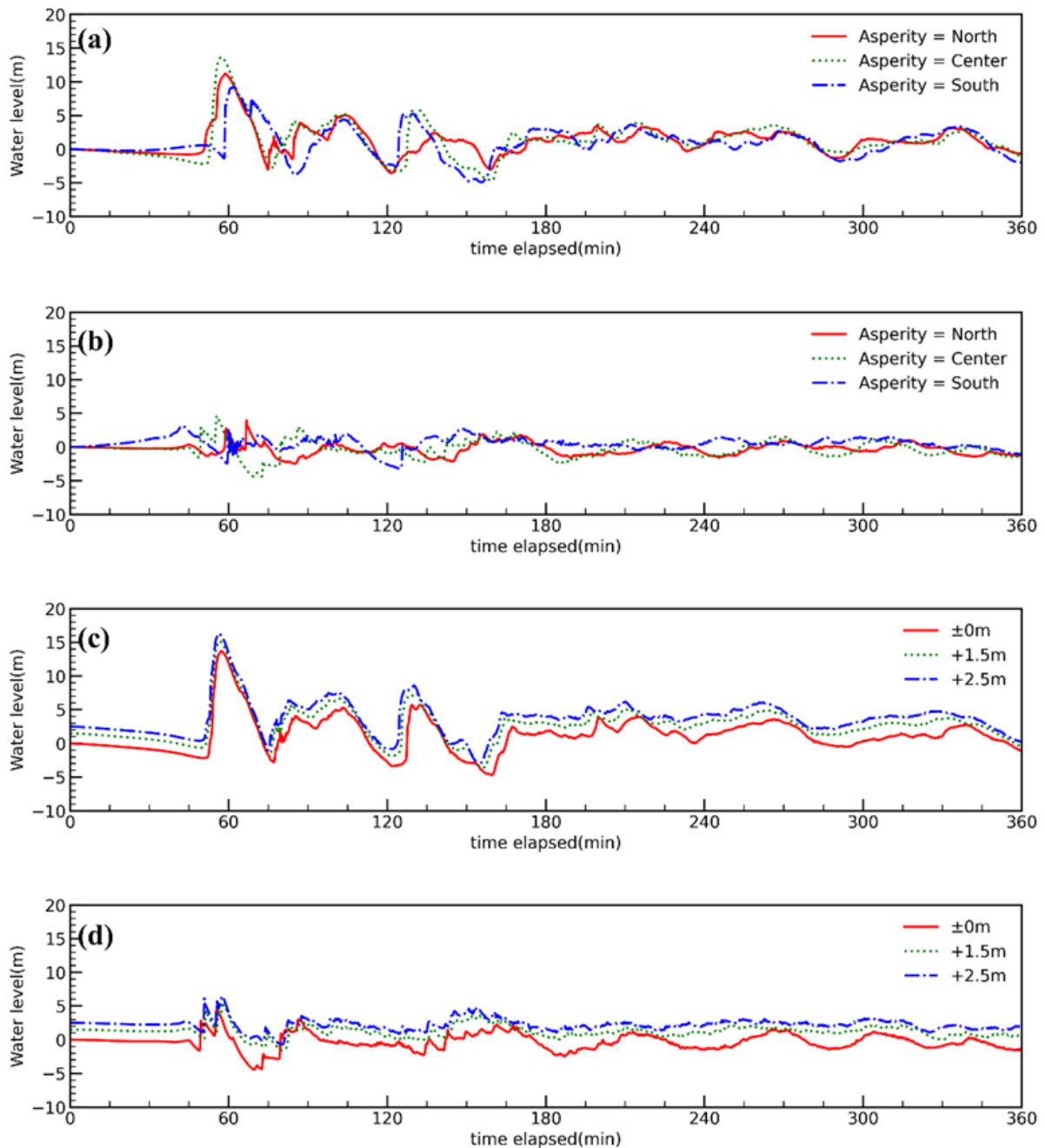
Figure 7. Time history of water surface elevations at the digital water buoys (a) off Sendai New-Port and (b) off Asahi City, based on earthquakes with Mw 9.1 and 3 different asperities being considered. (c) time history of water surface elevations for different SLR scenarios off Sendai New-Port and (d) off Asahi city.

3.2 Hazard curves at Sendai New Port and Kujukuri Beach

In this section, the fractile hazard curve of tsunami heights at the digital water buoys which were positioned at the same place as the actual tide gauge off the Sendai New Port and offshore of Asahi City are presented, for both present day conditions and SLR scenarios (see Figure 6). At the tide gauge off the Sendai New Port, the actual maximum heights of the *2011 Tohoku Earthquake* and Tsunamis were at least 6.6 m (the tide gauge was broken after it recorded this value). The corresponding return period was found to be 1,472 years from the 5% fractile curve with the 50% and 95% fractile curves estimated to be 754 years and 590 years, respectively shown in Figure 8. Although the actual return period of the *2011 Tohoku Earthquake* is estimated to be 600 years (Fujiwara et al. 2013), the equivalent return period in the present analysis were found at the 95% fractile curve. However, the authors would like to state that the maximum heights of actual tsunamis could be higher. Using the obtained fractile curves, the tsunami heights with a return period of 1,000

years (i.e., a Level 2 tsunami, against which evacuation countermeasures are presently being designed in Japan) were compared for present day and future conditions. Figure 8 shows that a Level 2 tsunami at present has a range of 5.6 m to 11.7 m (from the 5% and 95% fractile curves), which would increase to 5.8 m - 12.0 m (for +0.5 m SLR) and to 6.8 m – 13.2 m (for +1.5 m SLR). The result at +2.5 m SLR has a range of 7.4 m to 14.0 m. The results of the arithmetic average curves show that the tsunami heights with a return period of 1,000 years at the digital water buoy off Sendai New-Port increased by 0 m to 0.4 m less than the water level increase in SLR scenario, as per the finding explained earlier in Section 3.1.
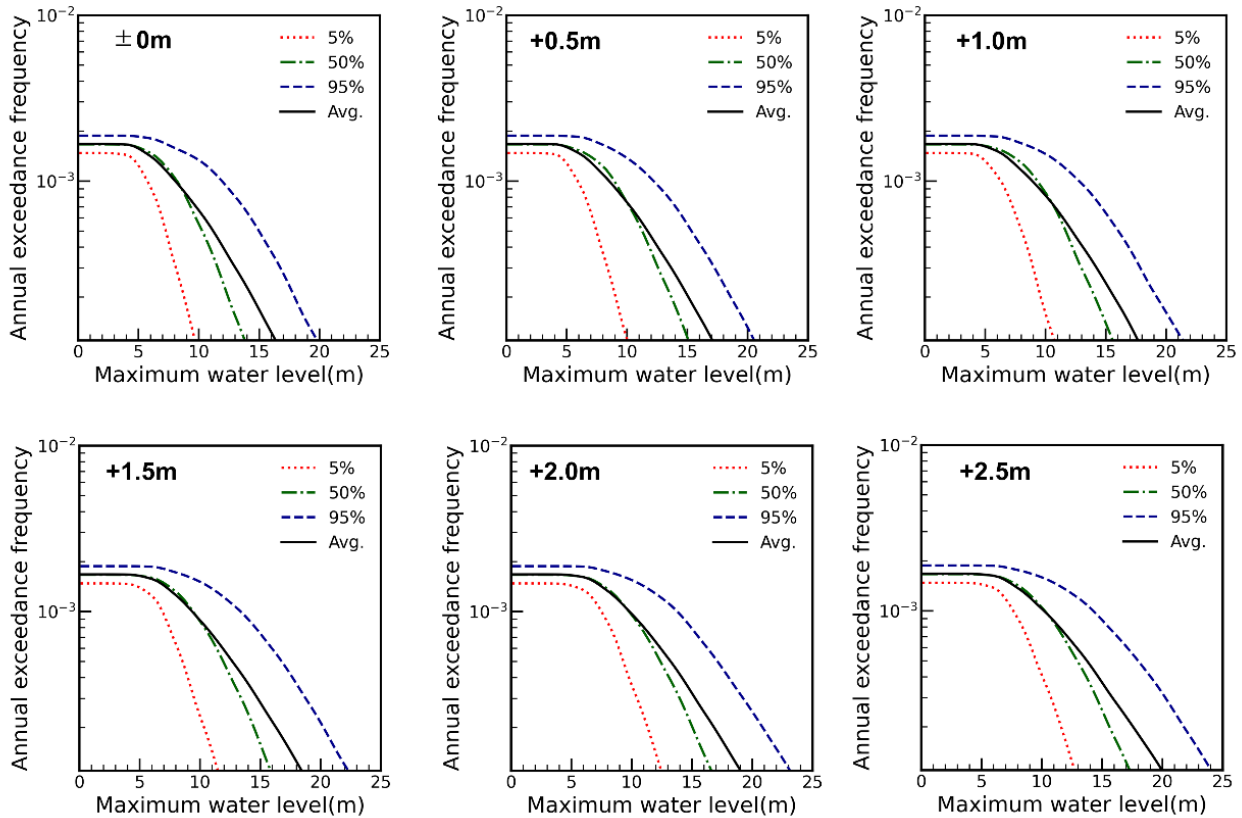

Figure 8. Fractile hazard curves (5%, 50%, 95% and their arithmetic average) of tsunami heights off Sendai New-Port based on SLR of between 0 m and 2.5 m.

The tsunami heights with a return period of 1,000 years (i.e., a Level 2 tsunami) were compared for present day and future conditions at the digital water buoy off Asahi City. Figure 9 shows how the maximum tsunami water levels for the present day, ranging from 2.4 m to 3.9 m (for the 5% and 95% fractile curves), would increase to 2.9 m - 4.6 m (for +0.5 m SLR), and 3.8 m - 5.6 m (for +1.5 m SLR). The results for a +2.5 m SLR scenario have a range of 4.7 m to 6.5 m (for the 5% and 95% fractile curves). Thus, all the results indicate that the increase in tsunami height exceeded the increase in the sea level, confirming the importance of performing tsunami simulations to more accurately address the SLR effects on the propagation and inundation of tsunamis. It is also worth mentioning that the tsunami heights ranges of 90% confidence interval (the distance between 5% and 95% fractile curves) at the output point off the Asahi City were 4.6 m to 5.0 m narrower than the results at the output point off the Sendai New-Port for each scenario.

Figure 10 shows the hazard curves (showing how the return period for given tsunami heights would change according to the SLR scenario considered), obtained from the average fractile curve at the two locations. The hazard curve for a 5 m tsunami off Sendai New-Port shows a moderate change, with a 660 and 636 years return period for the present day and +2.5 m SLR scenario, respectively. However, for 7.5 m and 10 m tsunami heights the return periods became more significantly shorter for the higher SLR scenarios. Significant change was also found at off Asahi City for higher tsunami. For example, the return periods for a 5 m tsunami height at off Asahi City change from 3,377 years to 1,116 years for the present day to +1.5 m SLR scenario, respectively).
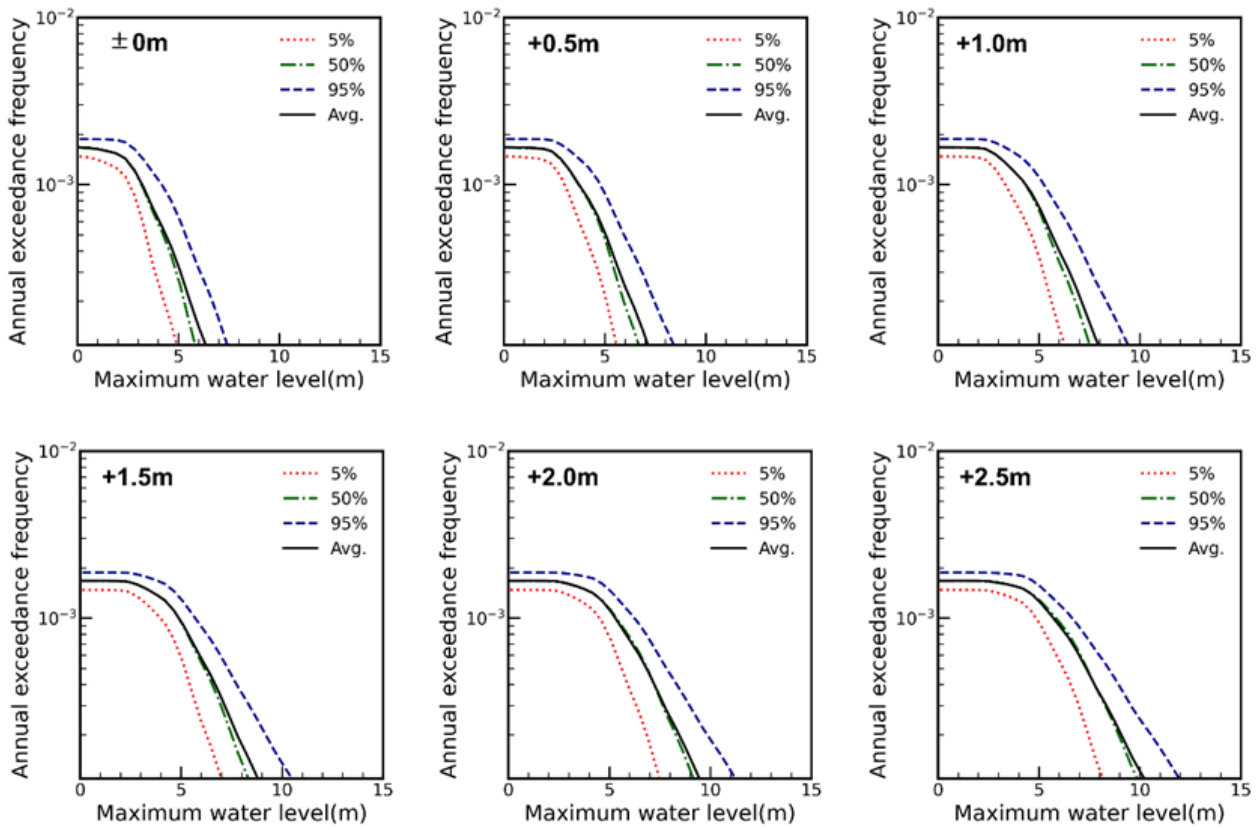
Figure 9. Fractile hazard curves (5%, 50%, 95% and their arithmetic average) of tsunami heights at off the Asahi City based on SLR scenarios of between 0m to 2.5m.
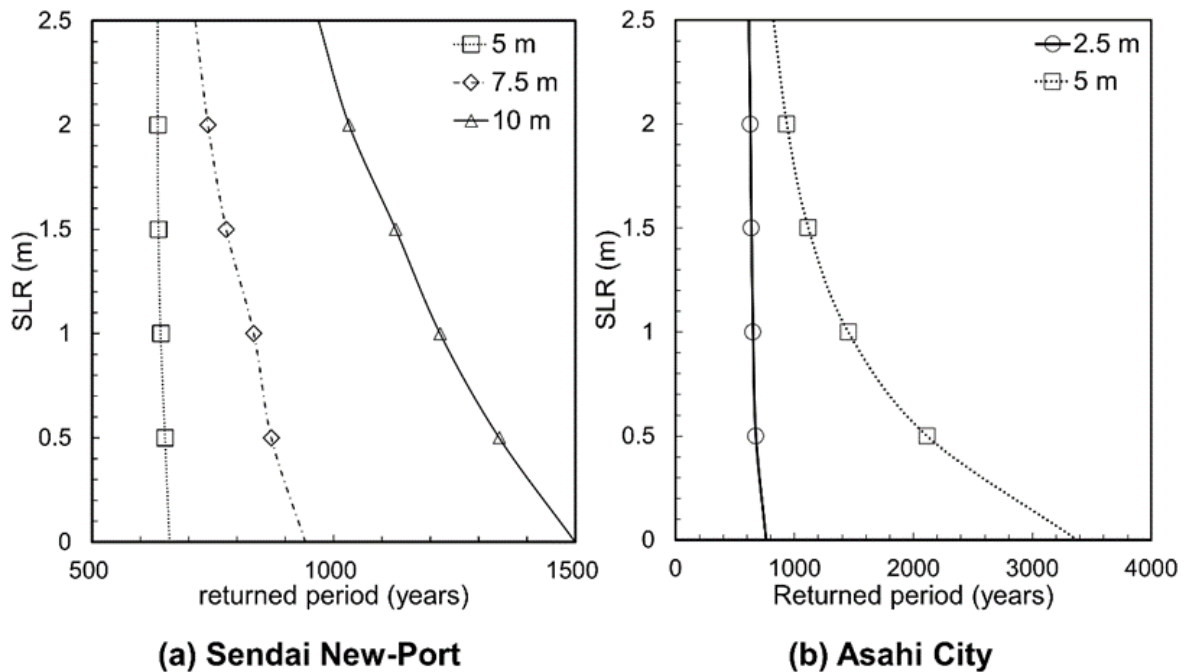

Figure 10. Hazard curves at (a) off Sendai New-Port and (b) off Asahi City for different SLR scenarios.

3.3 Tsunami heights along the eastern part of the Kanto Region

Figure 11 shows the distribution of tsunami heights with a return period of 1,000 years (i.e., a Level 2 tsunami) at the 10 m deep digital water buoys (output points) along the eastern part of the Kanto Region are compared, for each SLR scenario (for the 90% confidence intervals). The increase in maximum water level for the +0.5 m SLR scenario exceeds 0.5 m at

over 64% of output points, indicating that there are some nonlinear effects involved (plus possibly some other effects due to the slightly changed coastal geography). Specifically, the increase at output points along the northern part of Kanto region (point A) and the southern part of the Kujukuri Beach (points U and V) reached nearly 1.0 m. Such nonlinear effects were also observed for the +1.5 m (the increase in 50% of output points was greater than 1.5 m) and of +2.5 m SLR scenarios (35.7% of output points).

The 90% confidence intervals at most output points became narrower from the present day to +1.5 m SLR scenario. For instance, those around the northeastern coastline of the Kanto Region (points A to D) and the middle part of Kujukuri Beach (point P) narrowed by over 1.0 m. The amount of the change in 90% confidence interval differed according to the locations. Notably, the changes in the 90% confidence interval around Asahi City (point J) were 0.8 m to 1.9 m smaller than the averaged change along all the other points. Thus, the results suggest that the uncertainty in tsunami hazard would also change nonlinearly according to SLR scenarios.

4   Discussion

The results of this study show that the effect that SLRs has on potential tsunami heights is not linear, and could differ according to incorporation of initial wave heights and location. In this probabilistic model, SLRs were incorporated as an initial condition. The study by Adams et al. (2015) indicated the probability that the flow depths exceeds a specified level when the initial water level is sufficiently higher. According to the results of higher SLRs, the amounts of the sea water amplifying were non-linear, which could show the effect of initial water height setting. Offshore of Sendai New-Port, for the case of the earthquakes whose asperity was located in the central parts of the 2011 Tohoku Earthquake, the tsunami heights were higher than the ones in the earthquakes whose asperity was located in the northern or southern part. Tsunami heights at Asahi City showed the same trends for all asperities, which could be due to three reasons. First, the bathymetry around the cape in Asahi City could influence the transmission of waves from the east direction and cause refraction and the concentration of tsunami energy. Second, the continental shelf that is present along Kujukuri Beach can cause edge waves to be generated (see Koyano et al., 2021). Finally, the canyon located at the central part of the continental shelf along Kujukuri Beach could influence tsunami heights (see Figure 6). Essentially, when a continental shelf has a canyon, wave heights at both side of it can amplified, while the run-up directly behind the canyon is comparatively low (Aranguiz & Shibayama, 2013), which was corroborated in the present study.

It is important to also note that as a consequence of a major earthquake land subsidence can take place, and the *2011 Tohoku Earthquake* and *Tsunami* caused such a phenomenon along a wide stretch of the Tohoku coastline. Land subsidence of up to - 1.14 m was recorded at Ishinomaki city (Imakiire & Koarai, 2012), which lead to widespread problems for coastal infrastructure (Cao et al. 2020) and required extensive land elevation of coastal settlements (Esteban et al. 2015). Such effects should also be taken into account in simulations, though the *2011 Tohoku Earthquake* and *Tsunami* only caused modest subsidence in the case study area of the present research (-7 cm at Kujukuri Beach and -31 cm at Sendai New-Port), and hence was excluded from the present simulations.

The authors also would like to stress some of the limitations of this study. First, maximum water levels were considered as the only indicator to estimate the hazard against a Level 2 tsunami. While a logic tree approach can consider epistemic and aleatory uncertainties, it cannot estimate other important parameters such as the distributions of flow velocities. The use of a random phase model, which is a probabilistic model that models two-dimensional distributions of slip faults due to a random variation of phases in a spatial distribution of fault slips (see Goda et al., 2016), could also be used to further clarify the effects of SLRs, as this approach can provide the information about flow velocities. Finally, it is also worth mentioning that the present work only considers tsunamis generated in the same zone as that of the *2011 Tohoku Earthquake* (M_w 9.0), though other types of earthquakes along the Japan Trench should also be investigated. to make a comprehensive assessment of the hazards along the target coastline. In fact, earthquakes having smaller magnitudes (such as the *1896 Sanriku Earthquake Tsunami*, with an estimated magnitude of 8.2) are also known to have generated tsunamis along the Tohoku coast. Including such smaller earthquake-induced events would improve the accuracy of the estimated return periods for smaller tsunami heights.
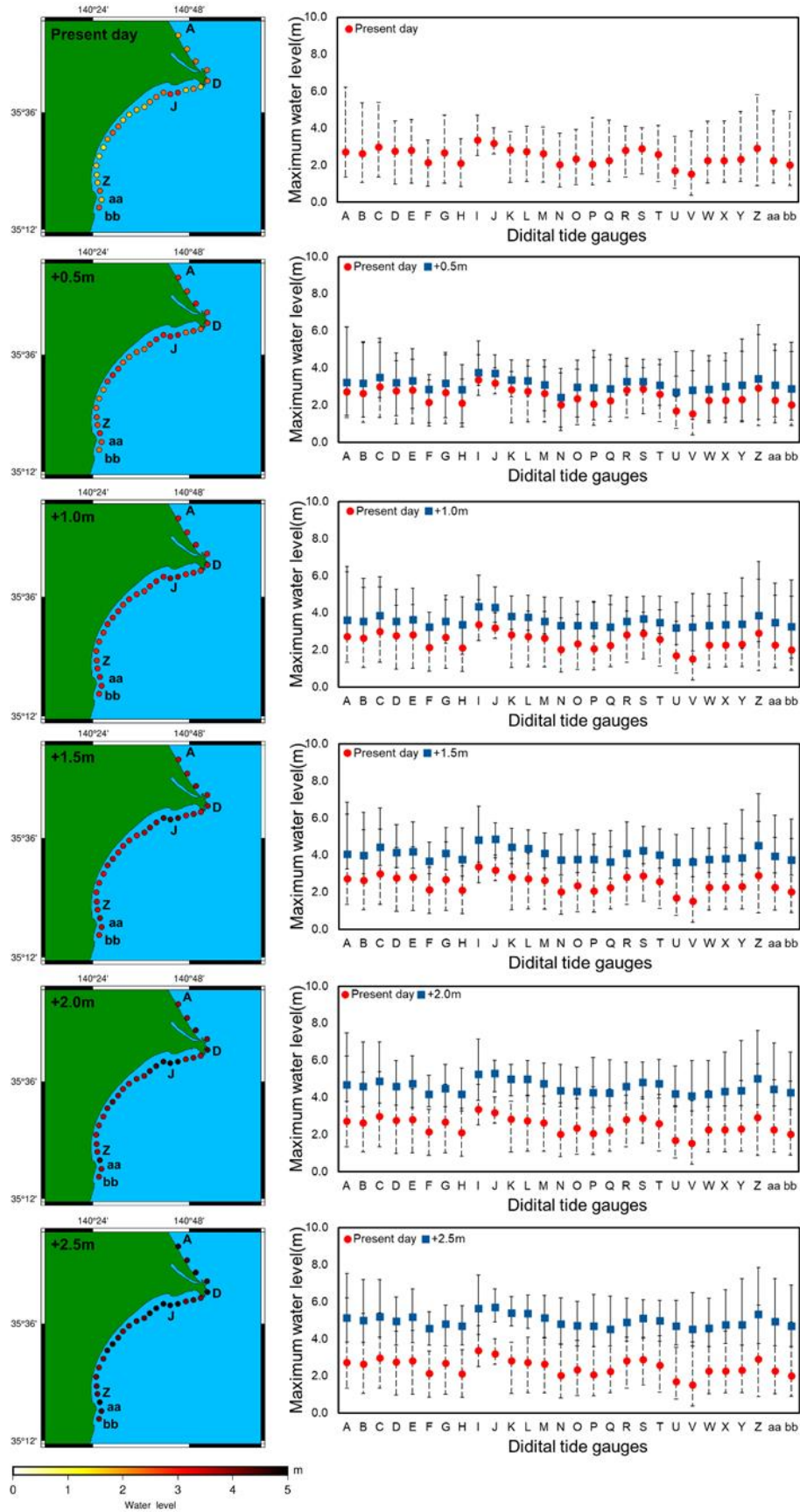
Figure 11. Left) Distribution of the maximum water levels for Level 2 tsunamis at digital the digital water buoys along the eastern part of Kanto Region (from the results of the average hazard curves), Right) The maximum water levels at these gauges, for the 90% confidence interval.

5   Conclusion

The 2011 Tohoku Earthquake and Tsunami and the 2018 Sulawesi Tsunami highlighted how tsunami damage can exceed the expectations of coastal disaster risk managers. As indicated in the present research, the design of countermeasures against Level 1 and 2 tsunamis will have to include the potential future effects of SLR, which might not be linear and vary according to location. The results showed that the expected tsunami heights and 90% confidence intervals changed nonlinearly due to the various SLR scenarios. For example, the increase in maximum water level exceeded 0.5 m at over 85% of output points for the +0.5 m SLR (this effect was especially pronounced for the northern part of Kanto region and the southern part of the Kujukuri Beach, there the increase reached nearly 1.0 m). A notable exception was around Asahi city, where the increase was smaller than other output points.

In the present work the expected Level 2 tsunami heights at output points offshore of Sendai New-Port and Asahi City were compared, indicating that the uncertainty on tsunami heights at Asahi City is lower than the one at the off Sendai New-Port. According to the hazard curves the return periods became significantly shorter for the higher SLR scenarios (for example, the return periods for a 5 m tsunami height offshore of Asahi City change from 11,070 to 2,027 years for the present day and +1.5 m SLR scenario, respectively). Thus, it appears to be important for coastal risk managers to consider the effects that SLR will have on the design of coastal protection structures, in order to choose appropriate design heights that reflect how expected risk levels will change in the course of the 21st century.

Acknowledgements

Author contributions (CRediT)

KK: Conceptualization, methodology, investigation, simulation, editing, data curation, manuscript writing and visualization. TT: Analysis, manuscript draft review and editing ME: Analysis, manuscript draft review and editing TS: Analysis, manuscript draft review and editing.

Notation

Name	Symbol	Unit
Average displacement across the fault	D	km
Seismic moment	M_0	N $\cdot$ m
Modulus of rigidity	ω	N/m^2
Fault area	S	km^2
Moment magnitude	Mw	N $\cdot$ m
Water surface elevation	η	m
Total water depth	D	m
Flux discharge in two horizontal directions	M, N	m^2/s
Manning's roughness coefficient	n	-
Gravity acceleration	g	m^2/s

References

Adams, L.M., LeVeque, R.J. & González, F.I. The Pattern Method for incorporating tidal uncertainty into probabilistic tsunami hazard assessment (PTHA). Nat Hazards 76, 19–39 (2015). https://doi.org/10.1007/s11069-014-1482-z

Aida, I. (1978). Reliability of a tsunami source model derived from fault parameters. Journal of Physics of the Earth, 26(1), 57–73. https://doi.org/10.4294/jpe1952.26.57

Annaka, T., Satake, K., Sakakiyama, T., Yanagisawa, K., & Shuto, N. (2007). Logic-tree approach for Probabilistic Tsunami Hazard Analysis and its applications to the Japanese coasts. Pure and Applied Geophysics, 164(2–3), 577–592. https://doi.org/10.1007/s00024-006-0174-3

Aranguiz, R., & Shibayama, T. (2013). Effect of submarine canyons on tsunami propagation: A case study of the biobio canyon, Chile. Coastal Engineering Journal, 55(4). https://doi.org/10.1142/S0578563413500162

Arnaud, G. E., Krien, Y., Abadie, S., Zahibo, N. and Dudon, B. (2021) How would the potential collapse of the Cumbre Vieja Volcano in La Palma Canary Islands impact the Guadeloupe Islands? Insights into the consequences of climate change. Geosciences, 11 (2) 56.

Becerra, I., Aránguiz, R., González, J., & Benavente, R. (2020). An improvement of tsunami hazard analysis in Central Chile based on stochastic rupture scenarios. Coastal Engineering Journal. https://doi.org/10.1080/21664250.2020.1812943

Cao, V. Q. A., Esteban, M. and Mino, T. (2020) Adapting wastewater treatment plants to sea level rise: Learning from land subsidence in Tohoku, Japan, Natural Hazards, 103, 885-902.

Cornell, C. A. (1968). Engineering seismic risk analysis. Bulletin of the Seismological Society of America, 58, 1588–1606.

Department of disaster management Chiba Prefecture. (2015). Damage report Chiba prefecture(in Japanese). Retrieved August 11, 2020, from https://www.pref.chiba.lg.jp/bousai/h23touhoku/20150501.html

Eshelby, J. D. (1957). The determination of the elastic field of an ellipsoidal inclusion, and related problems. Proceedings of the Royal Society of London. Series A. Mathematical and Physical Sciences, 241(1226), 376–396. https://doi.org/10.1098/rspa.1957.0133

Esteban, M., Onuki, M., Ikeda, I and Akiyama, T. (2015) "Reconstruction Following the 2011 Tohoku Earthquake Tsunami: Case Study of Otsuchi Town in Iwate Prefecture, Japan" in Handbook of Coastal Disaster Mitigation for Engineers and Planners. Esteban, M., Takagi, H. and Shibayama, T. (eds.). pp 615-630. Butterworth-Heinemann (Elsevier), Oxford, UK

Fujii, Y., Satake, K., Sakai, S., Shinohara, M., & Kanazawa, T. (2011). Tsunami source of the 2011 off the Pacific coast of Tohoku Earthquake. Earth, Planets and Space, 63(7), 815–820. https://doi.org/10.5047/eps.2011.06.010

Fujiwara. H, Kawai. S, Aoi. S, Morikawa. N, Senna.S, Azuma. H, Ooi. M, Hao. KX, Hasegawa. N, Maeda. T, Iwaki A, Wakamatsu. K, Imoto. M, Okumura. T, Matsuyama. H, N. A. (2013). Some improvements of seismic hazard assessment based on the 2011 Tohoku earthquake. Retrieved from https://dl.ndl.go.jp/info:ndljp/pid/9682770

Fukutani, Y., Moriguchi, S., Kotani, T., & Terada, K. (2018). Probabilistic tsunami loss estimation using response-surface -method application to Sagami Trough Earthquake. Journal of Japan Society of Civil Engineers, Ser. B2 (Coastal Engineering), 74(2), I_463-I_468. https://doi.org/10.2208/kaigan.74.i_463

Fukutani, Y., Suppasri A., Abe, Y., & Imamura, F. (2014). Stochastic Evaluation of Tsunami Inundation and Quantitative Estimating Tsunami Risk. Journal of Japan Society of Civil Engineers, Ser. B2 (Coastal Engineering), 70(2), I_1381-I_1385. https://doi.org/10.2208/kaigan.70.i_1381

Fukutani, Y., Suppasri A., & Imamura, F. (2015). Stochastic analysis and uncertainty assessment of tsunami wave height using a random source parameter model that targets a Tohoku-type earthquake fault. Stoch Environ Res Risk Assess, 29, 1763-1779. https://doi.org/10.1007/s00477-014-0966-4Goda, K., Mai, P. M., Yasuda, T., & Mori, N. (2014). Sensitivity of tsunami wave profiles and inundation simulations to earthquake slip and fault geometry for the 2011 Tohoku earthquake. Earth, Planets and Space, 66(1), 105. https://doi.org/10.1186/1880-5981-66-105

Goda, K., & Song, J. (2016). Uncertainty modeling and visualization for tsunami hazard and risk mapping: a case study for the 2011 Tohoku earthquake. Stochastic Environmental Research and Risk Assessment, 30(8), 2271–2285. https://doi.org/10.1007/s00477-015-1146-x

Harnantyari, A. S., Takabatake, T., Esteban, M., Valenzuela, P., Nishida, Y., Shibayama, T., … Kyaw, T. O. (2020). Tsunami awareness and evacuation behaviour during the 2018 Sulawesi Earthquake tsunami. International Journal of Disaster Risk Reduction, 43, 101389. https://doi.org/10.1016/j.ijdrr.2019.101389

Headquaters for Earthquake Research Promotion. (2020). Probabilistic Hazard Assessment of Tsunami due to Large Earthquakes along the Nankai Trough. Retrieved from https://www.jishin.go.jp/main/chousa/20jan_tsunami/nankai_tsunami.pdf (in Japanese)

Imamura F (1989) Tsunami numerical simulation with the staggered leap-frog scheme (numerical code of TUNAMI-N1). School of Civil Engineering, Asian Institute of Technology and Disaster Control Research Center, Tohoku University

J.A. Church, P.U. Clark, A. Cazenave, J.M. Gregory, S. Jevrejeva, A. Levermann, M.A. Merrifield, G.A. Milne, R.S. Nerem, P.D. Nunn, A.J. Payne, W.T. Pfeffer, D. S. and A. S. U. (2013). Sea Level Change. In Jan Lenaerts. Retrieved from Jan H. van Angelen website: http://www.climatechange2013.org/images/report/WG1AR5_Chapter13_FINAL.pdf

Japan Society of Civil Engineers (JSCE). (2002). Tsunami Assessment Method for Nuclear Power Plants in Japan. Retrieved from https://committees.jsce.or.jp/ceofnp/system/files/JSCE_Tsunami_060519.pdf

Japan Society of Civil Engineers (JSCE). (2008). Questionnaire survey of the weights on the logic-tree. Retrieved from http://committees.jsce.or.jp/ceofnp/system/files/Questionare_RT_PTHA_20141009_0.pdf

Japan Society of Civil Engineers (JSCE). (2011). Methods for Probabilistic Tsunami Hazard Assessment. Retrieved from https://committees.jsce.or.jp/ceofnp/system/files/PTHA20111209_0.pdf (in Japanese)

Japan Society of Civil Engineers (JSCE). (2016). Tsunami Assessment Method for Nuclear Power Plants in Japan 2016. Retrieved from https://committees.jsce.or.jp/ceofnp04/system/files/TAM2016_main_202010.pdf

Kawai, H., Satoh, M., Kawaguchi, K., & Seki, K. (2013). Characteristics of the 2011 Tohoku Tsunami waveform acquired around Japan by NOWPHAS equipment. Coastal Engineering Journal, 55(3). https://doi.org/10.1142/S0578563413500083

Kopp, R. E., DeConto, R. M., Bader, D. A., Hay, C. C., Horton, R. M., Kulp, S., … Strauss, B. H. (2017). Evolving Understanding of Antarctic Ice-Sheet Physics and Ambiguity in Probabilistic Sea-Level Projections. Earth's Future, 5(12), 1217–1233. https://doi.org/10.1002/2017EF000663

Kopp, R. E., Horton, R. M., Little, C. M., Mitrovica, J. X., Oppenheimer, M., Rasmussen, D. J., ⋯ Tebaldi, C. (2014). Probabilistic 21st and 22nd century sea‐level projections at a global network of tide‐gauge sites. Earth's Future, 2(8), 383−406. https://doi.org/10.1002/2014ef000239

Kotani, T., Tozato, K., Takase, S., Moriguchi, S., Terada, K., Fukutani, Y., … Choe, Y. (2020). Probabilistic tsunami hazard assessment with simulation-based response surfaces. Coastal Engineering, 160, 103719. https://doi.org/10.1016/j.coastaleng.2020.103719

Koyano, K., Takabatake, T., Esteban, M., & Shibayama, T. (2021). Influence of Edge Waves on Tsunami Characteristics along Kujukuri Beach, Japan. Journal of Waterway, Port, Coastal, and Ocean Engineering, 147(1), 04020049. https://doi.org/10.1061/(ASCE)WW.1943-5460.0000617

Kukita, S., & Shibayama, T. (2012). SIMULATION AND VIDEO ANALYSIS OF THE 2011 TOHOKU TSUNAMI IN KWSENNUMA. Journal of Japan Society of Civil Engineers, Ser. B3 (Ocean Engineering), 68(2), I_49-I_54. https://doi.org/10.2208/jscejoe.68.i_49

Lane, E.M., Gillibrand, P.A., Wang, X. et al. A Probabilistic Tsunami Hazard Study of the Auckland Region, Part II: Inundation Modelling and Hazard Assessment. Pure Appl. Geophys. 170, 1635–1646 (2013). https://doi.org/10.1007/s00024-012-0538-9

Li, L., Switzer, A. D., Wang, Y., Chan, C. H., Qiu, Q., & Weiss, R. (2018). A modest 0.5-m rise in sea level will double the tsunami hazard in Macau. Science Advances, 4(8), eaat1180. https://doi.org/10.1126/sciadv.aat1180

Mikami, T., Shibayama, T., Esteban, M., Takabatake, T., Nakamura, R., Nishida, Y., … Ohira, K. (2019). Field Survey of the 2018 Sulawesi Tsunami: Inundation and Run-up Heights and Damage to Coastal Communities. Pure and Applied Geophysics, 176(8), 3291–3304. https://doi.org/10.1007/s00024-019-02258-5

Mori, N., Mai, P. M., Goda, K., & Yasuda, T. (2017). Tsunami inundation variability from stochastic rupture scenarios: Application to multiple inversions of the 2011 Tohoku, Japan earthquake. Coastal Engineering, 127, 88–105. https://doi.org/10.1016/j.coastaleng.2017.06.013

Nagai, R., Takabatake, T., Esteban, M., Ishii, H., & Shibayama, T. (2020). Tsunami risk hazard in Tokyo Bay: The challenge of future sea level rise. International Journal of Disaster Risk Reduction, 45, 101321. https://doi.org/10.1016/j.ijdrr.2019.101321

National Police Agency of Japan. (2020). Damage report national police agency Japan(In Japanese). Retrieved August 4, 2020, from https://www.npa.go.jp/news/other/earthquake2011/pdf/higaijokyo.pdf

National Research Institute for Earth Science and Disaster Resilience. (2013). Japan Seismic Hazard Information Station: Hazard map of the probabilistic seismic motion. Retrieved August 28, 2020, from http://www.j-shis.bosai.go.jp/map/JSHIS2/download.html?lang=jp%3E

Nobuoka, H., & Onoue, Y. (2017). Comparison on capacity of Probabilistic hazard Analysis from high frequency to low frequency. Journal of Japan Society of Civil Engineers, Ser. B2 (Coastal Engineering), 73(2), I_1495-I_1500. https://doi.org/10.2208/kaigan.73.i_1495

Okada, Y. (1985). Surface deformation due to shear and tensile faults in a half-space. In Bulletin of the Seismological Society of America (Vol. 75).

Park, H., Alam, M. S., Cox, D. T., Barbosa, A. R., & van de Lindt, J.W. (2019). Probabilistic seismic and tsunami damage analysis (PSTDA) of the Cascadia Subduction Zone applied to Seaside, Oregon. International Journal of Disaster Risk Reduction, 35, 101076. https://doi.org/10.1016/j.ijdrr.2019.101076

Park, H., & Cox, D. T. (2016). Probabilistic assessment of near-field tsunami hazards: Inundation depth, velocity, momentum flux, arrival time, and duration applied to Seaside, Oregon. Coastal Engineering, 117, 79-96. https://doi.org/10.1016/j.coastaleng.2016.07.011

Park, H., Cox, D. T., Alam, M. S., & Barbosa, A. R. (2017). Probabilistic Seismic and Tsunami Hazard Analysis Conditioned on a Megathrust Rupture of the Cascadia Subduction Zone. Frontiers in Built Environment, 3, 32. https://doi.org/10.3389/fbuil.2017.00032

Shibayama, T., Esteban, M., Nistor, I., Takagi, H., Thao, N. D., Matsumaru, R., … Ohira, K. (2013). Classification of Tsunami and Evacuation Areas. Natural Hazards, 67(2), 365–386. https://doi.org/10.1007/s11069-013-0567-4

Somerville, P., Irikura, K., Graves, R., Sawada, S., Wald, D., Abrahamson, N., … Kowada, A. (1999). Characterizing crustal earthquake slip models for the prediction of strong ground motion. Seismological Research Letters, 70(1), 59–80. https://doi.org/10.1785/gssrl.70.1.59

Spence, R., Palmer, J., & Potangaroa, R. (2009). Eyewitness reports of the 2004 Indian Ocean tsunami from Sri Lanka, Thailand and Indonesia. Geotechnical, Geological and Earthquake Engineering, 7, 473–495. https://doi.org/10.1007/978-1-4020-8609-0_30

Sugino, H., Iwabuchi, Y., Abe, Y., & Imamura, F. (2015). Effect of the Modeling Method for Scenario Tsunami on the Probabilistic Tsunami Hazard Assessment. Journal of Japan Association for Earthquake Engineering, 15(4), 4_40-4_61. https://doi.org/10.5610/jaee.15.4_40

Sugino, H., Iwabuchi, Y., Hashimoto, N., Matsusue, K., Ebisawa, K., Kameda, H., & Imamura, F. (2014). The Characterizing Model for Tsunami Source regarding the Inter-plate Earthquake Tsunami. Journal of Japan Association for Earthquake Engineering, 14(5), 5_1-5_18. https://doi.org/10.5610/jaee.14.5_1

Takabatake, T., Fujisawa, K., Esteban, M., & Shibayama, T. (2020). Simulated effectiveness of a car evacuation from a tsunami. International Journal of Disaster Risk Reduction, 47, 101532. https://doi.org/10.1016/j.ijdrr.2020.101532

Takabatake, T., Shibayama, T., Esteban, M., Achiari, H., Nurisman, N., Gelfi, M., … Kyaw, T. O. (2019a). Field survey and evacuation behaviour during the 2018 Sunda Strait tsunami. Coastal Engineering Journal, 61(4), 423–443. https://doi.org/10.1080/21664250.2019.1647963

Takabatake, T., St-Germain, P., Nistor, I., Stolle, J., & Shibayama, T. (2019b). Numerical modelling of coastal inundation from Cascadia Subduction Zone tsunamis and implications for coastal communities on western Vancouver Island, Canada. Natural Hazards, 98(1), 267–291. https://doi.org/10.1007/s11069-019-03614-3

Teh, S. Y., Koh, H. L., Moh, Y. T., De Angelis, D. L., & Jiang, J. (2011). Tsunami risk mapping simulation for Malaysia. WIT Transactions on the Built Environment, 119, 3–14. https://doi.org/10.2495/DMAN110011

The 2011 Tohoku Earthquake Tsunami Joint Survey (TTJS) Group. (2012). Results of Tsunami surveys. Retrieved September 4, 2020, from https://coastal.jp/ttjt/

The Central Disaster Management Council(CDMC). (2006). Report of the Committee for Technical Investigation on Countermeasures for Earthquakes around the Japan Trench and the Kuril-Kamchatka Trench. 55. Retrieved from http://www.bousai.go.jp/kaigirep/chuobou/senmon/nihonkaiko_chisimajishin/pdf/houkokusiryou2.pdf

The Central Disaster Management Council(CDMC). (2011). The intermediate summary of the countermeasures following the 2011 Tohoku Earthquake. 21. Retrieved from http://www.bousai.go.jp/kaigirep/chousakai/tohokukyokun/pdf/tyuukan.pdf

Tursina, Syamsidik, Kato, S. and Afifuddin, M. (2021) Coupling sea-level rise with tsunamis: Projected adverse impact of future tsunamis on Banda Aceh city, Indonesia, International Journal of Disaster Risk Reduction, 55, 102084.

Wang, L., Huang, G., Zhou, W., & Chen, W. (2016). Historical change and future scenarios of sea level rise in Macau and adjacent waters. Advances in Atmospheric Sciences, 33(4), 462–475. https://doi.org/10.1007/s00376-015-5047-1

Yanagisawa, H., & Sasaki, K. (2015). The Validity of The Design Tsunami Height and Tsunami Risk Ranking in The Kamaishi Area. Journal of Japan Society of Civil Engineers, Ser. B2 (Coastal Engineering), 71(2), I_1585-I_1590. https://doi.org/10.2208/kaigan.71.i_1585

Youngs, R. R., & Coppersmith, K. J. (1985). Implications of fault slip rates and earthquake recurrence models to probabilistic seismic hazard estimates. Bulletin of the Seismological Society of America, 75(4), 939–964.

Appendix A. Fractile Hazard Curves

   Fractile hazard curves were created based on the tsunami hazard curves obtained from the numerical simulations and cumulative weights. An ergodic hypothesis is assumed to define the variation in tsunami heights (an ergodic hypothesis is a hypothesis where the variation of time and spatial domain are equivalent). In this study, Aida's κ and the standard deviation of log-normal distribution σ represent the variation in the spatial and time domain, respectively. Consequently, a tsunami hazard curve (an annual probability of exceedance) can be created. The weight on the each of the branches of the logic-tree determines the probable rate of occurrence of the scenarios based on the questionnaire survey of earthquake and tsunami experts and error evaluations, and each value is linked to different tsunami hazard curves as shown in the Figure A1a. At each tsunami height, different annual probabilities can be estimated and the distribution function of weights for each tsunami height can be obtained (as shown in Figure A1b). According to the distribution function of weights, the cumulative distribution function of weights can be obtained, as shown in Figure A1c. Fractile hazard curves can then be obtained by estimating the annual exceedance probability of different cumulative distribution function of weights.
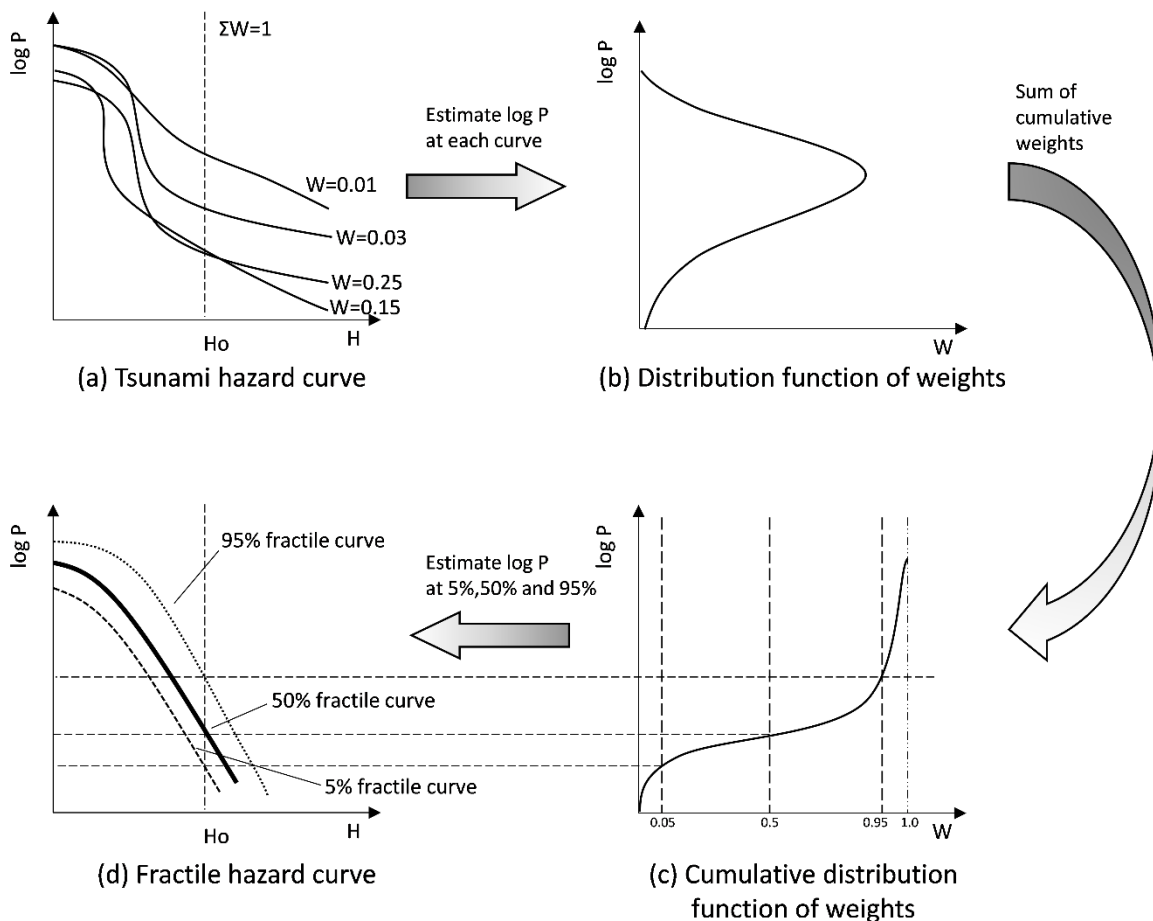
Figure A1. Calculation process of fractile hazard curves (created after Figure 5.3.6-1 in JSCE [2016]).

References

Japan Society of Civil Engineers (JSCE). (2016). Tsunami Assessment Method for Nuclear Power Plants in Japan 2016. Retrieved from https://committees.jsce.or.jp/ceofnp04/system/files/TAM2016_main_202010.pdf